Organotypic culture of post-mortem adult human brain explants exhibits synaptic plasticity

Yukiko Iwasaki, Corentin Bernou, Barbara Gorda, Sophie Colomb, Gowrishankar Ganesh, Raphael Gaudin

Organotypic culture of post-mortem adult human brain explants exhibits synaptic plasticity

Yukiko Iwasaki[1,2,3,*], Corentin Bernou[1,3,*], Barbara Gorda[1,3], Sophie Colomb[1,4], Gowrishankar Ganesh[1,2,#], Raphael Gaudin[1,3,#]

[1] Univ Montpellier, Montpellier, France.

[2] UM-CNRS Laboratoire d'Informatique de Robotique et de Microelectronique de Montpellier (LIRMM), 161, Rue Ada, Montpellier, France.

[3] CNRS, Institut de Recherche en Infectiologie de Montpellier (IRIM), 1919 route de Mende, Montpellier, France.

[4] Emergency Pole, Forensic Medicine Department, Montpellier University Hospital, 371 Avenue du Doyen Gaston Giraud, Montpellier, 34285, France.

* These authors contributed equally to this work

Co-corresponding authors:

Ganesh Gowrishankar Ganesh.Gowrishankar@lirmm.fr

Raphael Gaudin Raphael.Gaudin@irim.cnrs.fr

Short title: Synaptic plasticity in adult human brain explants

Keywords: central nervous system; cortex; local field potential; synaptic plasticity

Highlights:

- *Ex vivo* culture of *post-mortem* brain explants (OPAB) respond to electrical stimulation
- Induction of long-term potentiation in OPAB occurs upon multiday test/training phases
- Dopamine treatment prevents focalized long-term potentiation induction in OPAB

Abstract (150 words max)

Background: Synaptic plasticity is an essential process encoding fine-tuned brain functions, but models to study this process in adult human systems are lacking.

Objective/Hypothesis: We aim to test whether *ex vivo* organotypic culture of *post-mortem* adult brain explants (OPAB) retain synaptic plasticity.

Methods: OPAB were seeded on 3D microelectrode arrays to measure local field potential (LFP). Paired stimulation of distant electrodes was performed over three days to investigate our capacity to modulate specific neuronal connections.

Results: Long-term potentiation (LTP) or depression (LTD) did not occur within a single day. In contrast, after two and three days of training, OPABs showed a significant modulation of the paired electrodes' response compared to the non-paired electrodes from the same array. This response was alleviated upon treatment with dopamine.

Conclusion(s): Our work highlights that adult human brain explants retain synaptic plasticity, offering novel approaches to neural circuitry in animal-free models.

Introduction

The human brain is a highly organized tissue composed of an interwoven network of neural cells, in which information is transmitted through intercellular synaptic structures. The neuronal network conveys electric activity over long distances, and the strength of the pre/post-synaptic interactions is a critical parameter encoding neurological functions. Both murine and more recently cerebral organoid models have been instrumental in uncovering seminal paradigms, which however, could not be always transferable to the human brain, highlighting the need for complementary approaches (Mansvelder *et al*, 2019).

Hebbian plasticity postulates that paired stimulations of the pre- and post-synaptic compartments modulates the strength of synaptic connections, best exemplified in protocols of Spike-Timing Dependent Plasticity (STDP) (Bi & Poo, 1998; Brzosko *et al*, 2019). Such approaches induce either timing-dependent-long-term-potentiation (LTP) or -depression (LTD), according to the specific stimulations exerted. Numerous STDP-based studies have been performed in mouse models, but do not address the extensive differences between human and mouse brains (Hodge *et al*, 2019). Accordingly, STDP protocols induce very different outcomes depending on whether the sample is of human or mouse origin (Mansvelder *et al.*, 2019). Human induced pluripotent stem cells derived neurons represent a versatile model for assessing human neural plasticity and LTP *in vitro (Dong et al, 2020)*, but such approaches do neither recapitulate the diverse architecture of the human brain nor its complete cellular composition. STDP has been shown in human brain resections in patch-clamp settings (Verhoog *et al*, 2016), but induction of LTP or LTD in local field potential (LFP) and multi-electrode arrays (MEAs) remains challenging.

We recently characterized the *organotypic culture of human post-mortem adult brain explants* (OPAB), and recorded spontaneous electrical activity *ex vivo* using 3D microelectrode arrays (MEA) (Partiot *et al*, 2024). We showed that spontaneous LFP generated by OPAB can be exploited to characterize external perturbations, such as viral infections, using dedicated machine learning frameworks. However, intrinsic heterogeneity of the brain explants and absence of synchronicity lead to relatively high variability of the spontaneous LFP signal.

Hence, we investigated whether the *ex vivo* culture of human brain explants can exhibit Hebbian plasticity by applying a STDP protocol, and specifically paired stimulation electrodes. Although synaptic plasticity did not change significantly a couple of hours post-stimulation, we found that OPAB exhibited increased response the following days. Interestingly, treatment of the OPAB with Dopamine prevented such inter-day plasticity, which illustrated the fine-tuned regulation of this process.

Material and Methods

Ethics

The research presented in the study complies with all relevant ethical regulations. The protocol for the use of *post mortem* brain explants for research purposes included in this study was approved by the institutional review board (IRB) of the CHU of Montpellier (approval ID: 202000643) and the French Biomedicine Agency (agreement number PSF20-025). It permits human brain resection for research purposes during autopsy performed at the forensics institute of the CHU de Montpellier, upon obtaining local prosecutor authorization and family consent.

Donor enrolment

Excluding criteria were causes of death involving the head and neck (e.g. car crashes, stroke), and previously known severe neuropathology (e.g. epilepsy, neurodegenerative diseases). Altering substances (e.g. alcohol, opiates) were not included in selection criteria but are reported for each donor (**Supplementary Table S1**). Post-mortem interval for all selected donors was between 1 and 22 h. The data presented in this study originate from 9 donors aged 27 to 76 years old.

Brain slice preparation and culture

During autopsy, after incising and reclining the scalp, the skull was opened with an electric saw and the whole brain was extracted. Macroscopic examination attested to the absence of brain lesions, and a 2-3 cm thick coronal slice of the primary motor cortex (M1, frontal lobe) was dissected, and immediately transferred for transportation into cold medium containing 1X Neurobasal media (Thermofisher), supplemented with N2 (Gibco), 1X Glutamax (Thermofisher), and 0.5% Penicillin/Streptomycin (Thermofisher), hereafter referred to as N2 media. Samples were kept at 4°C during the transfer to the lab (< 30 min) to be processed. Under sterile conditions, the *dura mater* was removed, individual folds were isolated and embedded into 3% low melting-point agarose (Thermofisher). Slices of 300-µm thick were sectioned using a vibratome (PELCO Easyslicer, Ted Pella). Suitable slices were selected based on cytoarchitectural integrity of the cortical structure, i.e. presence of white matter and all layers of the gray matter. For culture, brain slices no younger than 5 days *in vitro* were transferred to an insert lifting a PET membrane with 0.4 µm pores (Sabeu), hanging over 2.5 ml of medium (changed every 2-3 days) in a 6-well plate. Slices were maintained at 37°C, 5% CO_2 and 95% humidity atmosphere.

Electrophysiology

For sensitive LFP measurement and stimulation of the tissue, OPAB were plated on 3D MEA (MultiChannel System), containing an array of 60 TiN-coated conical electrodes of 12 µm diameter

active site and 80 µm height, spaced by 200 µm each. The OPAB were transferred to MEAs the day prior to experiment using a brush and spatula, with the membrane side down, and the basal side of the cortex oriented towards the ground electrode. The OPAB were maintained in 150 µl BrainPhys aCSF (StemCell Technologies), supplemented with N2 and Glutamax. The medium was changed daily for up to 3 days post seeding, and individual MEAs were kept in a humidified petri dish to limit evaporation.

For recordings, MEAs were dried of any moisture on the connective parts and quickly transferred under a sterile hood onto a MEA2100-Mini headstage (MCS) connected to a digital amplifier (MCS). The headstage was shielded using tin foil and placed in an incubator at 37°C, 5% CO_2 and 95% humidity atmosphere for recording. LFP data was acquired at a 10 kHz sampling rate.

For selecting the electrodes for the experiment, first the most active electrodes were visually identified during a 2 min baseline recording prior to experiment. A 35 mV monophasic pulse was applied for 200 µs to one of the active electrode, and the response of the stimulation was assessed for electrodes separated by at least two electrodes. Once an electrode eliciting a response of more than 5 mV was isolated, it was next stimulated and we verified if this stimulation elicited a response (> 5 mV amplitude) in the first stimulated electrode. This process was repeated until 2 suitable electrodes eliciting responses (> 5 mV amplitude) on either direction was isolated. These were chosen for the paired stimulation experiment.

Paired stimulation protocol

The experiment extended over a period of three days. Correspondingly, we present the data labeled as being from 0 h (zero hour), 24 h (24 hours) and 48 h (48 hours), relative to the start of the recording. The MEA mounted OPAB were exposed to 9 stimulation blocks each day, comprising of 5 alternating 'test' blocks and 4 'training' blocks (starting with a test block).

Each training block consisted of 300 pairs of 1 Hz stimulations of the *stimulus-electrode* (orange electrode in **Fig. 1D**) followed by the stimulation of the *paired-electrode* (cyan electrode in **Fig. 1D**). We tested a few stimulation parameters (not shown) to converge on the currently used constant monophasic stimulation of 35 mV applied for 200µs, applied to both the stimulus-electrode and paired-electrode. In the training blocks, the two stimulations were applied with a time gap of 12 ms between them. In the test block, the same stimulation was applied only to the stimulus-electrode, 10 times, again at 1 Hz. We recorded the resulting *response* (defined later) in the paired-electrode from 10 ms prior to the stimulus-electrode stimulation till 90 ms after the stimulus-electrode stimulation. A period of 60 seconds separated each training and test block. Note that all the data in Figs 1 and 2 are

of the response of the paired-electrode area in the test blocks (block represented by numbers) over the three days (hours represented as subscript).

Treatment

In the dopamine-treated slices (10 slices from 5 donors), 10 µM Dopamine (Sigma-Aldrich) was added 2 min before the first test block. The dopamine treatment was performed while the MEA was on headstage, followed by gentle shaking. Slices were washed 3 times with aCSF 1 h after the end of the last test block every experiment day, in order to avoid over-night exposure of dopamine.

Imaging

Following the three days experiment, an OPAB were washed in phosphate buffered saline (PBS) and fixed in 4% paraformaldehyde (PFA) for 1 h at room temperature before staining. Samples were permeabilized with permeabilization buffer (0.5% BSA, 1% Triton in PBS) for 24 h on a rocker and all subsequent steps were performed in permeabilization buffer with overnight incubations. OPAB were labeled with primary rabbit polyclonal anti-MAP2 (GeneTex, #GTX133109), and chicken anti-MBP (Thermo Fisher Scientific, #PA110008) antibodies, washed and labeled with appropriate secondary antibodies; donkey anti-rabbit IgG Alexa Fluor Plus 488 (Thermo Fisher Scientific, #A-21206), donkey anti-chicken Alexa Fluor 647 (Jackson ImmunoResearch, #703-605-155) and Dapi nuclear counterstain (Pierce) at a final concentration of 1 µg/ml. For viability assessment, OPAB healthiness was assessed using the LIVE/DEAD Viability/Cytotoxicity kit (Thermofisher Scientific) for 30 min, washed in PBS and fixed in 4% paraformaldehyde (PFA) for 1 h at RT. Upon fixation, OPABs were fully immerged in RapiClear 1.52 reagent (Sunjin Lab) overnight at RT to clarify the samples before imaging. The images were taken on a spinning disk confocal microscope (Dragonfly, Oxford Instruments) equipped with an ultrasensitive 1024 x 1024 EMCCD camera (iXon Life 888, Andor) using the 405, 488 and 637 nm laser lines with a 40X NA 1.3 oil-immersion objective. Images were processed using Bitplane Imaris x64 (Oxford Instruments) version 9.7.

Data Analysis

Data was exported as ASCII files and analyzed using a custom MatLab/Octave (v8.4.0) script. The *stimulated area* (a 3x3 electrode group neighboring the *stimulus-electrode*), *paired area* (a 3x3 electrode group neighboring the paired-electrode) and ground electrode were excluded from background calculation. The *response* of the *paired-electrodes* was calculated by averaging the peak activation (after every stimulation of the stimulus-electrode) in the 9 electrodes of the paired area. The response in the *nonpaired electrodes* was calculated by averaging the peak activations across all the electrodes except those in the paired-area, the stimulated area and the ground electrode.

The response across the 5 test blocks (averaged over the 10 stimulations) is shown for each OPAB at 0 h (**Fig**. **2C**), 24 h (**Fig. 2D**) and 48 h (**Fig. 2E**) of the experiment. **Fig. 2F** shows the absolute difference in the response in the first test at 24 h from that of the first test of 0 h ($T_{24}0$ - $T_0 0$) in cyan from each OPAB. This is compared with the same difference in response ($T_{24}0$ - $T_0 0$) in the corresponding non-paired electrodes for each OPAB.

Fig. 2G shows a similar difference in first test responses between 48 h and 0 h ($T_{48}0$ - $T_0 0$) in the paired-electrode (cyan data) and non-paired electrodes (grey data). **Fig. 2H-I** show the same measures from the Dopamine treated slices.

Grubb's outlier test was used on each test and consistently removed two slices which had very high basal activation levels, one from the non-dopamine experiment, and one from the dopamine addition experiment. These two slices were excluded from the analysis and the data presented here altogether.

In addition, $Test_0 1$ of slice 9 in the non-dopamine experiment presented a technical issue, and the slice was removed from 1-way paired ANOVA analysis in **Fig. 2C**, but kept in all subsequent statistical analysis.

Statistical significance of within day trends was analyzed using a 1-way ANOVAs while the significance of response differences between the paired-electrode and nonpaired electrodes was assessed using Wilcoxon paired signed-rank test. Schemes were created with Biorender.com.

Results & Discussion

We have recently characterized the use of OPAB for antiviral assessment (Partiot *et al.*, 2024), and here we further confirm that OPAB contains neural cells including neurons, myelin and astrocytes, while exhibiting synaptic boutons (**Figure 1A-C**). Furthermore, the OPAB were found to produce spontaneous LFP, indicating that a subset of neural circuits has been preserved, despite the post-mortem collection of the tissue and the slicing procedure. Hence, we wondered whether the remaining synaptic connections showed plastic properties and endeavored to test the well-established protocol of coincidental stimulation, known to induce STDP. To this end, we performed training blocks of alternated training and test blocks (**Figure 1D)**, in order to induce plasticity between two distant areas of the slices. In the test block, the stimulation was applied only to the stimulus-electrode, while we recorded the response in the paired-electrode (**Fig. 1D** and Material & Methods).

The activation in the paired-electrode showed an increase, followed by a decrease, after which it slowly converged back to the baseline (**Fig. 2A**). We use the peak voltage of the increase (grey arrow) to quantify the response in each electrode. Heatmaps representing the response change over time as a function of electrode position across tests and days showed that the paired electrode tends to exhibit

higher response amplitude compared to non-paired electrodes (**Fig. 2B** and **Supplementary Fig. S1-S2**). Spatiotemporal quantitative analysis revealed that single-day training over the 4 training blocks was unable to trigger a significant change in the response, neither in the paired-electrode (**Fig. 2C**; F=1.033, p = 0.354, 1-way repeated measures ANOVA), nor in the non-paired electrodes (F = 2.331, p = 0.1215, not shown). We did however observe some OPABs showing either an increase or decreas in response across the day. To further ensure that intra-day changes were indeed absent, we also analyzed the unsigned intra-day changes by analyzing the absolute difference in response between the 4^{th} and 0^{th} test in the day over the paired-area (ie. abs ($T_0$4-$T_0$0)). We compared these absolute changes in the paired-area against similar measures in the non-paired area but found that there were no differences between the two on 0h (p=0.24, paired T-Test).

Next, to test whether the response could have longer kinetics, we repeated the train/test blocks 24 and 48 h after the initial test as schematized in **Fig. 1D**. Paired-electrode response across the test sessions after one day (**Fig. 2D**) or after 2 days (**Fig. 2E**) showed again no change in the responses within each day, both for 24 h (F = 1.217, p= 0.303, 1-way repeated measures ANOVA) as well as 48 h (F =1.639, p =0.2219, 1-way repeated measures ANOVA). Furthermore, again difference were also absent between the unsigned response changes between the paired and unpaired areas on both 24h (p=0.29, paired Wilcoxon test) and 48h (p=0.33, paired T-Test).

We thus decided to quantify the changes across days in the response by analyzing the difference between the responses in paired-electrode in the first test block on each day (**Fig. 2F-I**, cyan). We compared these values to the change in response in the non-paired electrodes (**Fig. 2F-I**, grey) . Although we did observe important inter-slice variability, there was a clear change in the response amplitude across the days. Of the 14 slices we trained, 10 exhibited an increase in the response amplitude across the training blocks, while 4 exhibited a decrease in the response amplitude across the training blocks (**Fig. 2F-G**). Of note, the absolute response change is shown here. We observed a significant increase in response in the paired-electrodes compared to the non-paired electrodes, both after 24 h (**Fig. 2F**, p = 0.0353, Wilcoxon paired signed Rank test) and after 48 h (**Fig. 2G**, p = 0.0031, Wilcoxon paired signed Rank test). Analysis of all the slices revealed that this increase occurred in 71% (24 h) and 79% (48 h) of slices (**Fig. 2F-G**). These findings indicate that our paired stimulation protocol can induce synaptic plasticity in OPAB, that become apparent over a multiday timescale.

Interestingly however, dopamine treatment during training (at 0 h) reverted the observed changes in response level (**Figure 2H-I**) (p = 0.0039, Wilcoxon paired signed Rank test), suggesting that in our model, dopamine prevents synaptic plasticity. This could be due to the preferential activation of inhibitory dopamine receptor classes (D2-4), which would hamper learning upon coincidental

stimulation. Further research using specific dopamine receptor agonists/antagonists is needed to determine their role in OPAB synaptic plasticity.

In conclusion, our study highlights that brain explants obtained *post-mortem* and cultured *ex vivo*, can show plasticity upon paired stimulation training. The design of this work did not aim at correlating how the timing of stimulation impacts the level of response induction (which could then be referred to as STDP), but rather to illustrate that a classical STDP-inspired experimental design of coincidental stimulation readily induces synaptic plasticity in the complex OPAB model. Seminal studies in human samples have previously compared various time-lags using patch clamp (Chen *et al*, 1996; Mansvelder *et al.*, 2019; Testa-Silva *et al*, 2010). While the rules governing STDP in human cortex remain incompletely understood and widely variable, our approach is likely to provide additional complexity to this issue, and future work shall specifically investigate how the time lag affect synaptic plasticity using MEA-based LFP.

Responses to the test/train protocol was variable, with some slices poorly responding to the stimulation. This could be due to the high inter-donor and inter-slice variability, as previously shown (Partiot *et al.*, 2024). Moreover, the intrinsic neural circuitry of each slice is relatively unique and it is likely that some of our test/train electrodes were not adequately connected to induce a STDP response. We chose to perform the more integrative approach of MEA-based LFP recording and stimulation, as this approach can represent a surrogate to current *in vivo* development of brain-machine interfaces (BMI) implanted in the brain of mice, monkeys and even humans (Neuralink).

Finally, we found that treatment with low concentration of dopamine prevents synaptic plasticity induction in OPAB. Although unexpected, our ability to modulate STDP in OPAB indicates that this model can readily be used to investigate modulators of synaptic plasticity. Previous work suggested that dopamine gates the induction of LTP in mice prefrontal cortex (Xu & Yao, 2010). This data contrasts with our findings, but may be explained by the difference of species, model, maturity, and specificity of the brain region. One could hypothesize that the developing cortex may favor the learning of new motor skills through overall dopamine-mediated system activation, whereas a mature motor cortex may be wired for learning fine motor skills, which may refine neuronal circuitry through inhibitory signals and fine-tuned functional reorganization. Such a switch in mouse STDP response has been shown to occur during development, hinting at dramatic changes in STDP outcome depending on the cellular context (Itami & Kimura, 2012; Kimura & Itami, 2019). Our OPAB model originates from adults, but the organotypic culture of post-mortem fetal human cortical brain explants would represent an attractive model to compare STDP and evaluate the pleiotropic functions of neuromodulators during development.

Author contribution

Conceptualization: GG, RG; Formal analysis: YI, CB; Funding acquisition: SC, GG, RG; Investigation: YI, CB, BG, GG, RG; Methodology: YI, CB, BG, SC, GG, RG; Project administration: GG, RG; Family consent & sample collection: SC; Software: YI, CB; Supervision: GG, RG; Visualization: YI, CB, RG; Writing - original draft: RG; Writing - review & editing: YI, CB, BG, CC, GG, RG.

Acknowledgments

We acknowledge the MRI imaging facility (CNRS, Univ Montpellier) for access, maintenance, training and advice on the microscopes.

Funding

This work was partially supported by the Agence Nationale de la Recherche [ANR-21-CE33-0007-03, to SC, GG and RG], and the ANR-MRSEI2023 grant to GG and RG.

Competing interests

Authors declare that they have no competing interests.

References

Bi GQ, Poo MM (1998) Synaptic modifications in cultured hippocampal neurons: dependence on spike timing, synaptic strength, and postsynaptic cell type. *J Neurosci* 18: 10464-10472

Brzosko Z, Mierau SB, Paulsen O (2019) Neuromodulation of Spike-Timing-Dependent Plasticity: Past, Present, and Future. *Neuron* 103: 563-581

Chen WR, Lee S, Kato K, Spencer DD, Shepherd GM, Williamson A (1996) Long-term modifications of synaptic efficacy in the human inferior and middle temporal cortex. *Proc Natl Acad Sci U S A* 93: 8011-8015

Dong Y, Xiong M, Chen Y, Tao Y, Li X, Bhattacharyya A, Zhang SC (2020) Plasticity of Synaptic Transmission in Human Stem Cell-Derived Neural Networks. *iScience* 23: 100829

Hodge RD, Bakken TE, Miller JA, Smith KA, Barkan ER, Graybuck LT, Close JL, Long B, Johansen N, Penn O *et al* (2019) Conserved cell types with divergent features in human versus mouse cortex. *Nature* 573: 61-68

Itami C, Kimura F (2012) Developmental switch in spike timing-dependent plasticity at layers 4-2/3 in the rodent barrel cortex. *J Neurosci* 32: 15000-15011

Kimura F, Itami C (2019) A Hypothetical Model Concerning How Spike-Timing-Dependent Plasticity Contributes to Neural Circuit Formation and Initiation of the Critical Period in Barrel Cortex. *J Neurosci* 39: 3784-3791

Mansvelder HD, Verhoog MB, Goriounova NA (2019) Synaptic plasticity in human cortical circuits: cellular mechanisms of learning and memory in the human brain? *Curr Opin Neurobiol* 54: 186-193

Partiot E, Gorda B, Lutz W, Lebrun S, Khalfi P, Mora S, Charlot B, Majzoub K, Desagher S, Ganesh G *et al* (2024) Organotypic culture of human brain explants as a preclinical model for AI-driven antiviral studies. *EMBO Molecular Medicine*

Testa-Silva G, Verhoog MB, Goriounova NA, Loebel A, Hjorth J, Baayen JC, de Kock CP, Mansvelder HD (2010) Human synapses show a wide temporal window for spike-timing-dependent plasticity. *Front Synaptic Neurosci* 2: 12

Verhoog MB, Obermayer J, Kortleven CA, Wilbers R, Wester J, Baayen JC, De Kock CPJ, Meredith RM, Mansvelder HD (2016) Layer-specific cholinergic control of human and mouse cortical synaptic plasticity. *Nat Commun* 7: 12826

Xu TX, Yao WD (2010) D1 and D2 dopamine receptors in separate circuits cooperate to drive associative long-term potentiation in the prefrontal cortex. *Proc Natl Acad Sci U S A* 107: 16366-16371

Figures & figure legends

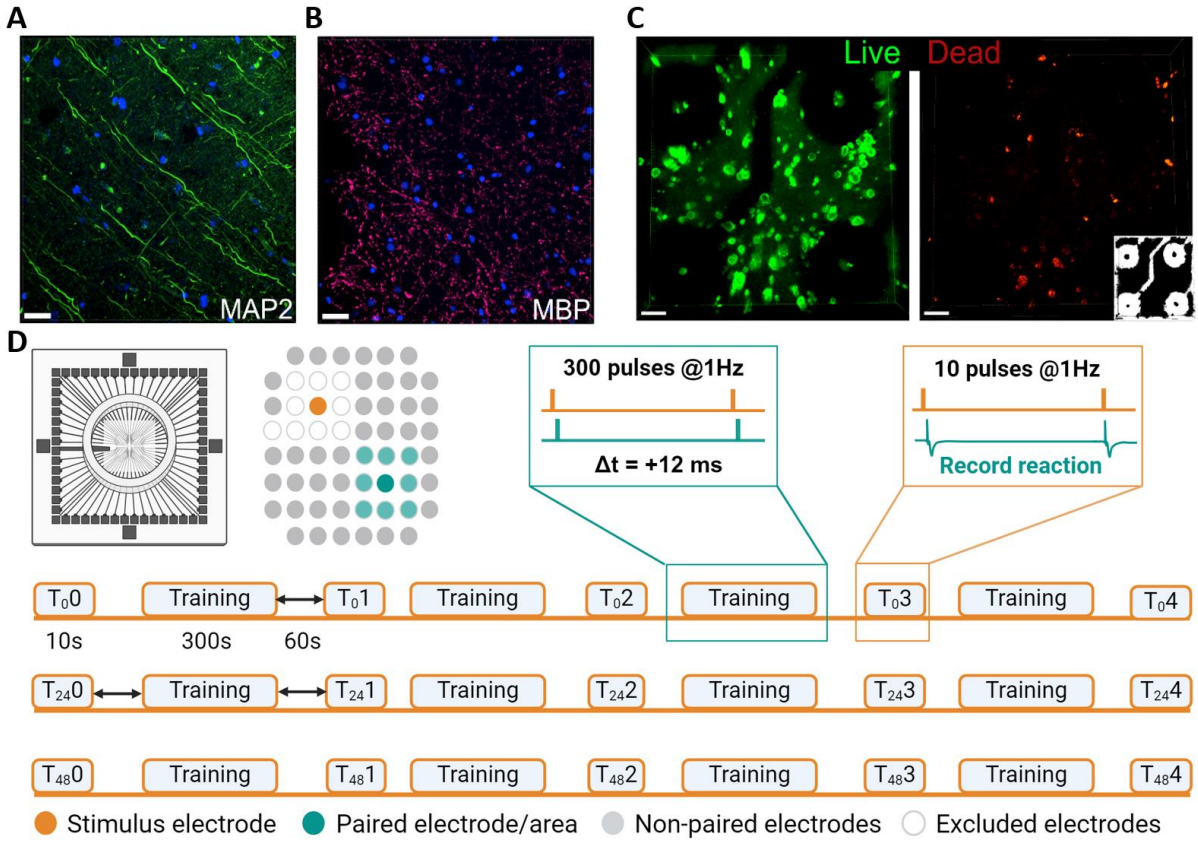

Figure 1. OPAB and the paired stimulation protocol. (**A-B**) Confocal microscopy of frontal OPAB, showing neurons (MAP2) and oligodendrocytes (MBP). Nuclei are visible through Dapi staining in blue. Images are representative of a 10 µm Z stack. Scale bar = 30 µm. (**C**) Confocal microscopy of a frontal OPAB laying on a 3D MEA and labeled with a Live/Dead marker, staining living cells in green (left), and dead cells in red (right). Scale bar = 30 µm. The micrographs highlight that many cells are alive. The lower right inset shows a saturated image of the same area, revealing the pattern of four electrodes (white). (**D**) top left panel shows the microelectrode array (MEA) and the cartoon of a stimulated electrode (orange), paired-electrode (dark cyan), the paired-area (light cyan) and the non-paired electrodes (grey). The area around the stimulus electrode and the ground (both in white). The right and bottom panels show the schematic representation of the 5 test blocks and 4 training blocks in the paired stimulation protocol. The protocol was repeated for three consecutive days. In the training blocks the stimulus electrode and paired electrodes were stimulated repeatedly with a time difference of 12 ms. In the test blocks, only the stimulus electrode was stimulated and we recorded the 'response' in the paired electrode.

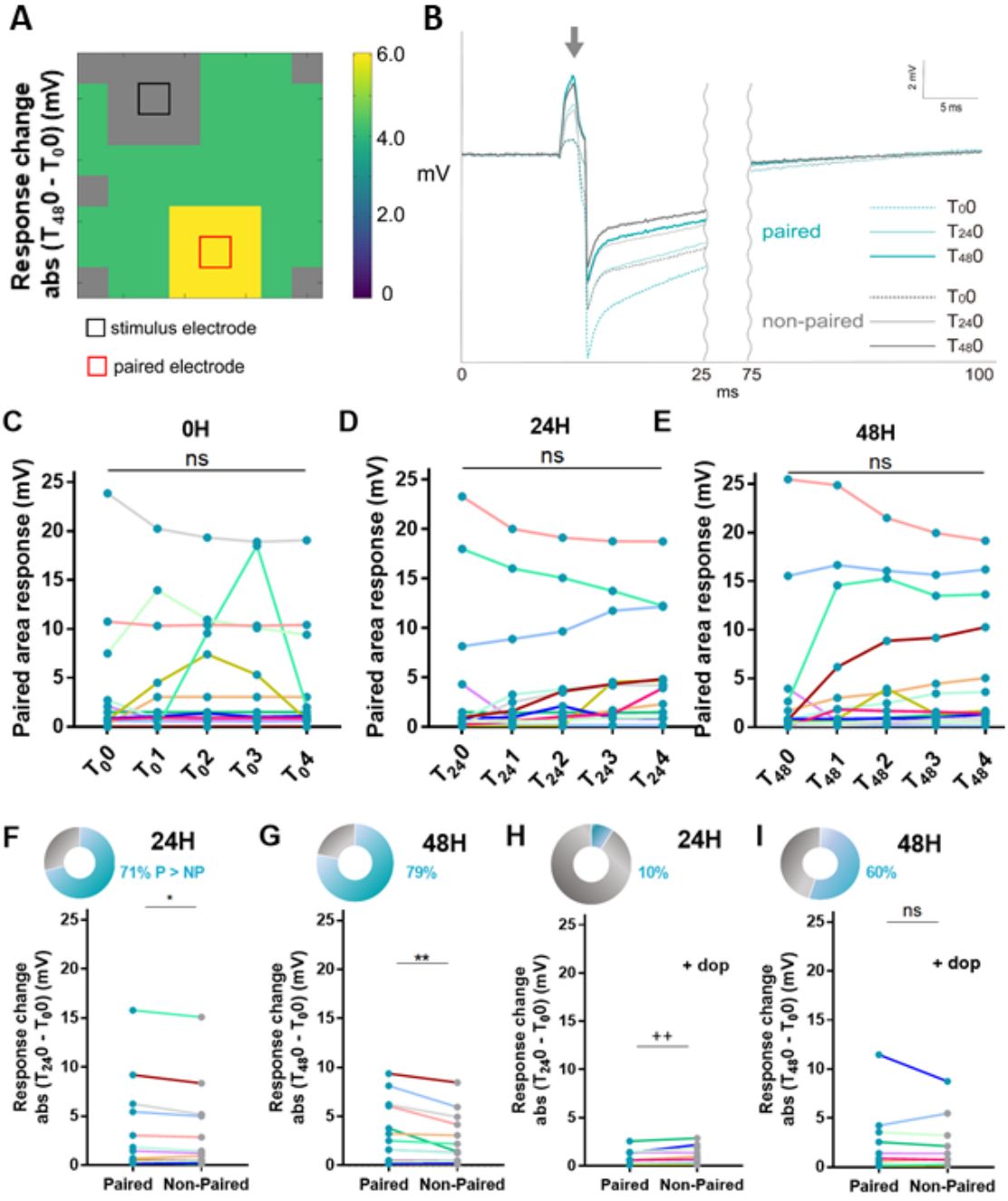

Figure 2. OPAB exhibit inter-day STDP. (**A**) Representative traces of the average recorded LFP in the paired area and non-paired area of one OPAB over the three days. (**B**) Representative heatmap of the average absolute response difference in the non-paired electrodes and paired area in one OPAB at $T_{48}0$. Grey: excluded/absent electrodes. Similar heat maps for 24 and 48 h from all the OPABs are provided as **Supplementary Fig. S1-S2**, respectively. (**C-E**) Response (calculated as the averaged peak activity across the paired-area) recorded across the test sessions on day 1 (0 h, **C**), day 2 (24 h, **D**) and day 3 (48 h, **E**). Each data point corresponds to an average of the n = 10 recordings in a test block. (**F-G**) Average absolute response change in the paired and non-paired electrodes at 24 h (abs ($T_{24}0 - T_0 0$), **F**) and 48 h (abs ($T_{48}0 - T_0 0$), **G**). A significantly higher response change was observed in paired electrodes compared to non-paired electrodes both at 24 H (p=0.035, Wilcoxon signed-rank test) and 48 h (p = 0.0031, Wilcoxon signed-rank test). (**F-I**) Pie inserts represent the proportion of OPABs with Paired > NonPaired (cyan) and Paired < Non-Paired (grey). (**C-G**) n= 14 slices from 9 donors. (**H-I**) To

examine the effect of dopamine, OPABs were treated with 10 μM dopamine during the first training block at 0 h. Dopamine treatment prevented a response change in the paired-electrode, with in fact the non-paired electrodes showing larger response change than the paired-electrode at 24 h (++: $p < 0.05$, Wilcoxon signed-rank test, **H**). No difference of response was observed between the paired-electrode and non-paired electrodes at 48 h (I). (**H-I**) n = 10 OPABs from 6 donors.

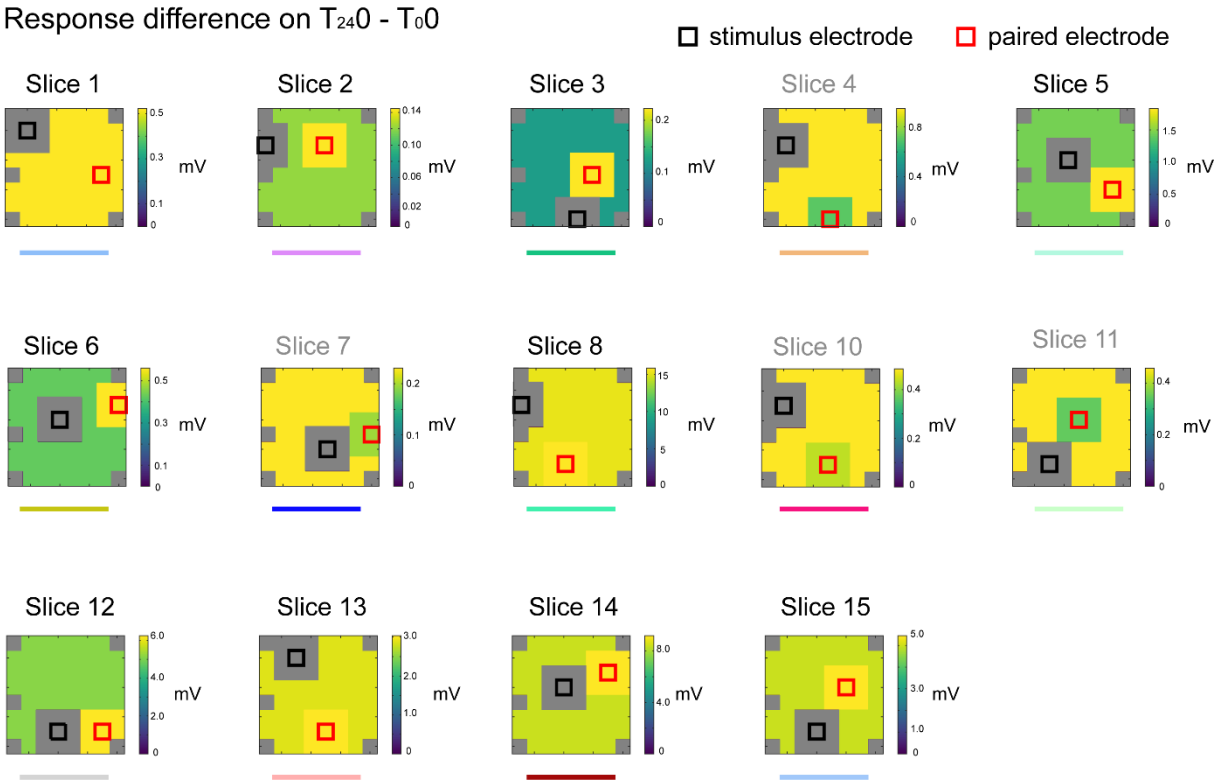

Supplementary Figure S1: Heatmaps of OPAB responses to stimulation at 24 h ($T_{24}0 - T_0 0$) show that paired-electrode (red square) and its surroundings (paired-area) had generally higher response than the average response in the non-paired electrodes. 9 out of 14 OPABs show a higher response at 24 h, and this number increased to 11 out of 14 at 48 h (see **Fig. S2**). The stimulus electrode is shown as a black square. The grey electrodes (electrodes neighboring the stimulus electrode, the ground electrode and the edges where there were no electrodes) were excluded from the response analysis.

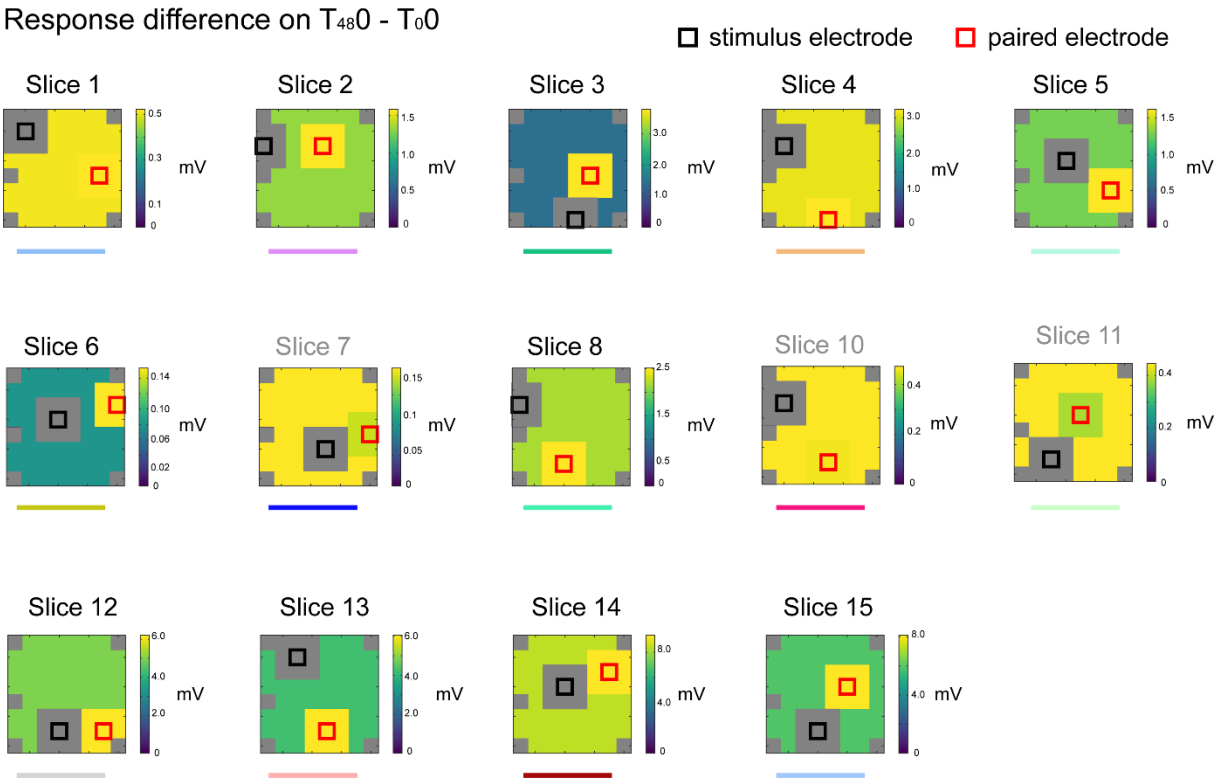

Supplementary Figure S2: Heat maps of OPAB responses to stimulation at 48 h ($T_{48}0 – T_00$).

Supplementary Table S1. Clinical data of the donors from which the OPAB were obtained.

	P1	P2	P3	P4	P5	P6	P7	P8	P9	P10	P11	P12
Sex (Male/Female)	M	F	M	F	F	M	M	M	M	F	M	F
Age	35	52	72	54	76	63	47	27	51	60	58	35
Delay post mortem	<9h	<6h	<12h	<6h	<1h	<1h	<5h	<1h	<6h	0	<4h	<22h
Cause of death	cardiological and/or toxicological	drug intoxication	Toxicological	Toxicological	acute decompensated respiratory and heart	heart attack	acute mesenteric ischemia	probably toxicological	probably toxicological	heart attack	pulmonary infection	probably toxicological
Known treatment	possibly opioids	possibly antidepressant, anti-anxiety	antidepressant, antimetabolites,anti-hypertensives,	possibly opioids	unknown	anti-hypertensives,	unknown	opioids, anti-anxiety.	possibly opioids		thyroïd substitutes	antipsychotic, anti-anxiety
Comorbidities	pancreatisis, chronic alcoholism,drug addiction	depression, fibromyalgia, shoulder algodystrophy	hypertension, tachycardia, chronic alcoholism	bipolar, chronic alcoholism	Respiratory and heart failure, breast cancer	hypertension, chronic alcoholism, heart failure	chronic alcoholism, smoking	drug addiction	drug addiction, chronic alcoholism	dyslipidemia, smoking	chronic alcoholism, smoking, heart and liver troubles	bipolar, suicide attempts
BMI	severe obesity	29	35	28	18	24	slim	20	34	30	15	34
Corticosteroid treatment	N	N	O	N	N	N	N	N	N	N	N	N